Aveen S. Abdulhamed
Qusay A. Abbas

Department of Physics, College of Science, University of Baghdad, Baghdad, IRAQ

Effect of Magnetic Field on Characteristics of Micro-Discharges Generated by Dielectric Barrier Discharge Actuator

The present work studied the influence of a parallel magnetic field on the properties of micro-discharges generated in a DBD actuator under atmospheric pressure. The micro-discharge is formed when the Ac high voltage with frequency of 9 kHz was applied. As well as, the magnetic parallel field was present when the magnetic permanent was putting behind the powered electrode. The micro-discharge characteristics were measured at various horizontal distance that varying for 0 to 5 cm. Magnetic field effects on micro-discharge properties at different horizontal distances were examined. The results indicated that the influence of the powered electrode area affect the micro-discharge. The presence of the parallel magnetic field shown inverse behavior on the micro-discharge characteristics.

Keywords: Micro-discharge; Optical Emission Spectra; Magnetized DBD; Actuators
Received: 29 January 2024; **Revised:** 06 March; **Accepted:** 13 March 2024

1. Introduction

The dielectric barrier discharge (DBD) is considered to be one of the most economically efficient non-thermal plasma sources among the different options available. This discharge is recognized for its efficacy in initiating chemical and physical processes that take place in gases [1]. In past few years, DBD has been extensively studied due to its application in many different areas. This type of discharge covers many applications such as material surface processing [2,3] and also applications in the environment and energy field, water treatment [4-8], agriculture [9-11], surface modification [12,13], biomedical sterilization [14-16], pollution control [17] and medicine [18,19]. The ability of these DBD applications lies in their capacity to produce highly reactive plasma using a simple reactor system, requiring low energy consumption, and operating at room temperature and atmospheric pressure [20,21]. DBD reactor is fundamentally composed of a series of electrodes, separated by at least one dielectric barrier. To generate the breakdown in gases between the electrodes, a high enough electric field must be applied. Therefore, this feature represents the advantage of DBD than the other conventional plasma generator sources [22]. Anyway, in various industrial applications, active flow control is necessary to improve efficiency of system efficiency or to less the environmental load [23]. Therefore, the mechanical actuators were used to achieve flow control [24]. In 1990, Roth et. al. [24] developed a new device for flow control. The DBD device was utilized as a plasma actuator. The non-thermal plasma actuator functions at air pressure and has various advantages over traditional flow control actuators. These include compact size, straightforward design, lightweight construction, rapid response, and the absence of mechanical components [25-27]. For decades plasma actuators have received attention for the barrier discharge of the AC surface [28-31]. Basic plasma properties of AC-SDBDPAs have been studied [27]. Non-thermal plasma actuators for flow control were illustrated in many applications for separation flow control [32–35] and noise reduction [36,37]. The Based operating principle of plasma actuator is the electrohydrodynamic phenomenon that formed due to the transfer of the ions momentum to neutral molecules by impact process. DBD and corona discharges represent the most common discharge that occurs in the plasma actuators [38]. Moreover, numerous endeavors have been made to enhance the control authority and reduce the power demands of DBD actuators. The range is from 2 to 4. In these studies, several parameter trends have been examined, such as the characteristics of the input alternating current voltage (e.g., amplitude, frequency, and waveform shape), material properties, and the design of the DBD device. The amplitude of the sinusoidal input voltage increases as the electrical power consumed by the DBD actuators increases, as 3.5 PV. Moreover, the dielectric barrier discharge actuators make a wall jet with speed range from 1to 6 m/s occurring at distance range from 0.5 to 1 mm above the dielectric surface. According to experimental results, the maximum produced velocities was approximately 8 m/s2, while according to numerical predictions indicate velocities approximately up to10 m/s2 [39]. Recently, different researchers were studied the influence of the magnetic field on the characteristics of the DBD actuator and the researchers observed that the permanent magnetic field gives an impression of the movement of electrons after the release of DBD in the gaseous insulation [40]. The influence of the magnetic field that produced by permanent magnet in

the normal direction of the electric field on DBD performance was investigated in reference [41]. Furthermore, another study examined the contrast between the behavior of DBD with and without a magnetic field in the air. The findings demonstrated distinct variations in various DBD characteristics, including; DBD plasma, discharge current, power dissipation, and more, when the magnetic field was present compared to when it was absent [42,43]. When the pulse repetition frequency of unipolar positive nanosecond pulsed DBD lowers from 1200 to 100 Hz, the discharge becomes more homogeneous. Furthermore, an equivalent outcome can be attained in presence of a parallel magnetic field [44].

Present work characterizes micro-discharges that formed in single DBD actuator with two AC frequency and at different horizontal distances. The characterization encompassed many parameters such as micro discharge volume, I-V curve, Debye length, electron number density, electron temperature, plasma parameter, and plasma frequency.

2. Methodology

This section describes the theoretical description of some plasma parameters of micro discharge that formed in the DBD actuator, like; electron number density (n_e), electron temperature (T_e), Debye length (λ_D), plasma parameter. (N_D), and plasma frequency. (ω_p). The electron temperature (T_e) is the fundamental plasma parameters which used to describe the plasma state. In this work, the Boltzmann plot was utilized to calculate electron temperature, as [45-46]:

$$\ln\left(\frac{I_Z\lambda_{ki,z}}{g_{k,z}A_{ki,z}}\right) = -\frac{1}{kT_e}E_{k,z} + ln\left(\frac{hcL_{nz}}{4\pi P_z}\right) \qquad (1)$$

where Z is the species-related ionization state, C is speed of light, k is Boltzmann constant, L is characteristic length of the plasma, h is Planck's constant, E_k is energy of the upper energy level k, g_k is degeneracy of the upper energy level k, P_Z species partition function in ionization stage Z, and I_Z is optically measured integrated intensity of a species in ionization stage Z are all included. By graphing the left-hand side of equation (1) against the upper-level energy of the species in the Z ionization phase, a linear relationship is observed. The slope of this line corresponds to electron temperature in electron volts.

There are many methods adjusted to calculated the electron number density, the Stark broadening method is used in this work. The electron number density was determined using the Stark broadening method [47-50]:

$$n_e(cm^{-3}) = \left[\frac{\Delta\lambda}{2\omega_s}\right] N_r \qquad (2)$$

where ω_s is the electron impact, $\Delta\lambda$ denotes the full width at half maximum of the line, N_r is the reference electron number density, that equal of 10^{16} cm^{-3} for neutral atoms and 10^{17} cm^{-3} for singly charged ions.

Debye length (λ_D) is a fundamental quantity of the plasma that represents its ability to shield out electric potentials that are applied to it. λ_D is determine of the sheath thickness or shielding distance which can determined as [45,46,50,51]:

$$\lambda_D = 7430(kT/n)^{1/2} \quad m, T \ in \ eV \qquad (3)$$

The plasma parameter (N_D) represent the number of charged particles in the Debye sphere which can calculated as [52,53]:

$$N_D = \frac{4\pi}{3}n\lambda_D^3 = 1.38\times10^6\frac{T_e^{\frac{3}{2}}}{\sqrt{n}} \qquad (4)$$

where T_e is the electron temperature (in K) and n is the plasma number density (in cm^{-3})

Plasma frequency (ω_p) can define as the electrons oscillation around the original positions inside the plasma as a results of the electric force that built up due to the electrons displacement. This parameter was calculated from [49,46]:

$$\omega_p = \left(\frac{n_0e^2}{\epsilon_0 m_e}\right)^{1/2} (rad/s) \qquad (5)$$

where ε_0 is vacuum permittivity, e is the electronic charged, n_0 is the electron number density and m_e is the electron mass

3. Experimental Part

Figure (1) displays the experimental arrangement of magnetized DBD actuator system. The system consists of two circular disc aluminum electrodes with diameter 9 cm and thickness of 1 cm. Both electric electrodes are submerged in a circular Teflon container to preclude electrical sparks at edges of the electrodes.

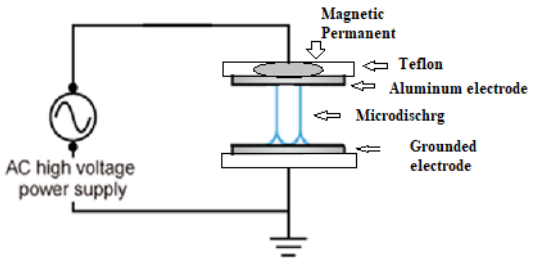

Fig. (1) Typical DBD actuator system

An AC high voltage (r.m.s is 22 kV) power supply with AC frequency of 9 kHz was supplied of one electrode, while the other electrode was connected to the ground. The distance between the two electrodes is 1cm and filled by air at atmospheric pressure at room temperature. One circular magnetic permanent (diameter of 7 cm and thickness of 1cm) was located inside the Teflon under the powered electrode in the parallel direction of the applied electric field. When the AC high voltage was supplied between two electrodes, a micro a discharge was established in the air gap between two electrodes in the absence and presence of the magnetic field. The micro-discharge generated in the DBD actuator is found by a high-resolution digital camera at various horizontal distances ranging from 0 to 5 cm. The emission spectra of the micro-discharge are recorded

using the THOR LAB model CCS100 optical emission spectrometer, manufactured in Germany. The measurements are conducted in two scenarios: one with the presence of a magnetic field and one without. The wavelength range for the recorded spectra is 320-740 nm. The magnetic field was measured by Leybold Tesla meter and has the value of 18.7 mT. The spectrometer was placed at an angle 45° from the direction of the magnetic field. The results of the emission spectra of the micro-discharge were adjusted with NIST database to determine the micro-discharge characteristics in the electrodes gap.

4. Results and Discussion

Figure (2) shows a photograph of such micro-discharges in air gap between electrodes at different horizontal distance in the lack of the magnetic field. Many features can be noted from this figure; the photographs display that the micro-discharge current is characterized by one distinct period of pulse, corresponding to the micro-discharge which due to streamer propagation.

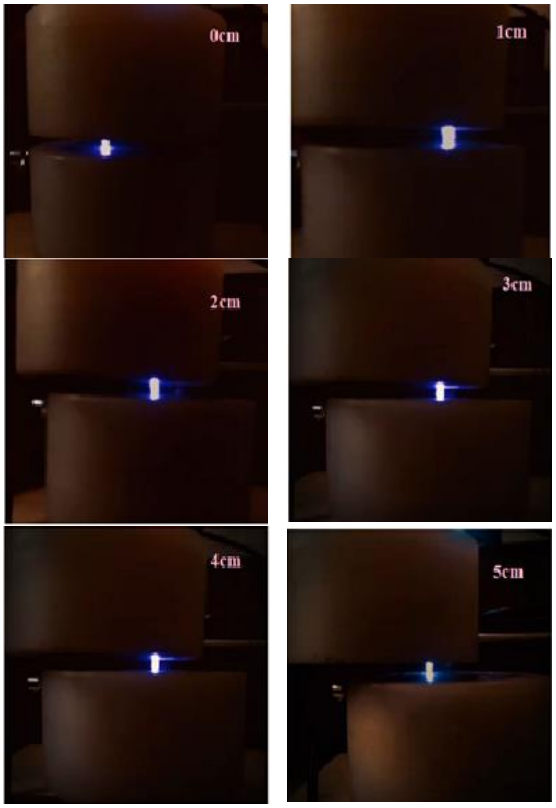

Fig. (2) Influence of horizontal distance on the micro-discharge that formed in DBD actuator in the absence of the magnetic field

Micro-discharges (sometimes called current filaments) generated from gases breakdown that occur at atmospheric pressure in DBD. These independent current filaments represent the most interesting property of DBDs. The temporal progression of the discharge current is significantly affected by multiple factors, which encompass the actuator's geometry, the electrical properties of the power supply, environmental conditions (such as humidity, pressure, temperature, and ambient gas), and the physicochemical attributes of the dielectric material. The second half of the paper will further explore the impact of geometry and electricity on the generated body force and subsequent electric wind [30].

The intensity of this micro- discharge depends strongly on the characteristics of AC power supply source. Increasing the horizontal distance from D equal 0 to 5 cm, the micro-discharge intensity increases. On the other hand, the effect of the magnetic field on the micro-discharge that formed in DBD actuator at different horizontal distances was demonstrated in Fig. (3). The illustration demonstrates the visible confirmation of the micro-discharge that takes place at the air gap between the electrodes. The magnetic field's presence influences the formation of micro-discharge in the air gap between the electrodes.

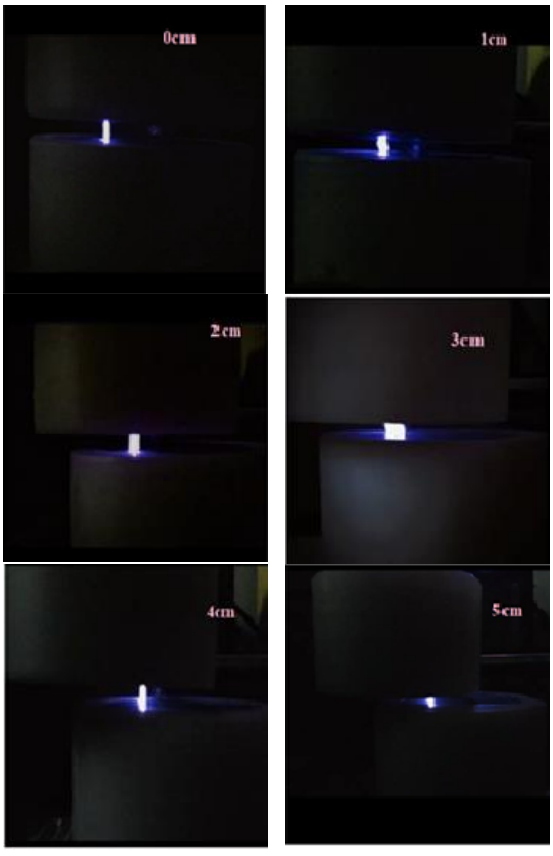

Fig. (3) Influence of horizontal distance on the micro-discharge that formed in DBD actuator in the Presence of the magnetic field

Plasma images of three models are depicted in Fig. (4). Upon comparing figures (2) and (3), it was seen that the micro-discharge created in the presence of the magnetic field exhibited a higher density compared to the micro-discharge formed in the absence of the magnetic field. The radiation emitted from plasma provides further information about

plasma characteristics [54,55]. Therefore, the optical emission spectroscopy (OES) technique is commonly employed for diagnosing of several types of laboratory plasma.

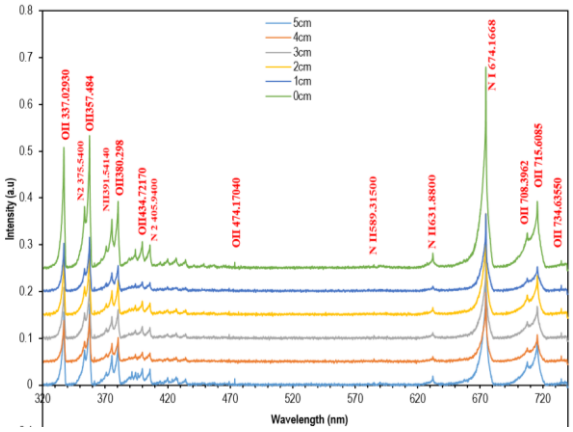

Fig. (4) Influence of horizontal distance on the emission spectra of micro-discharge in DBD actuator in the absence of the magnetic field

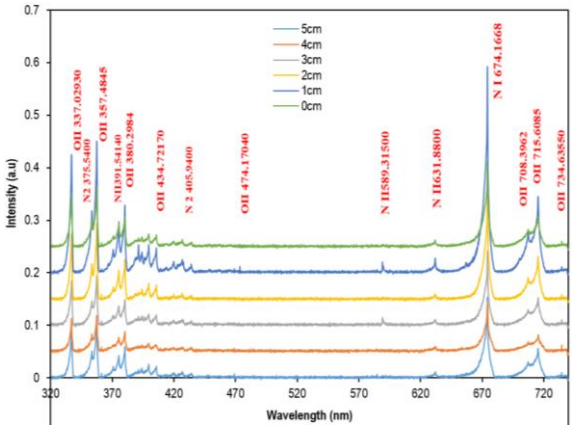

Fig. (5) Influence of horizontal distance on the emission spectra of micro-discharge in DBD actuator in the presence of the magnetic field

In the present work, OES approach was used to determine the characteristics of DBD actuator with and without magnetic field. The emission spectra of the micro- discharge that produced in the distance between the electrodes at normal atmospheric air pressure at wavelength range 320-740 nm in the presence and absence of the magnetic field is illustrated in figures (4) and (5), respectively. One can observed from these figures that there are many peaks of the ionic emission peaks of oxygen (OII) that appears at the wavelengths 337.029, 357.484, 380.298, 434.2003, 474.170, 708.3962, 715.608, and 734.635 nm. One atomic emission peak of nitrogen (NI) appear of wavelength of 674.167 nm and two ionic emission peaks of nitrogen (NII) detected at wavelengths of 391.541 and 631.880 nm. As well as, there are two molecular emission peaks of nitrogen (N2I) corresponding to wavelengths 375.540 and 405.940 nm. When moving the electrodes horizontally from 0 to 5cm, the results detected that intensity decreases as distance increases. This result agree with references [46,56]. Finally, the comparison of figures (4) and (5) shown that the emission lines intensity are increases in the presence of the magnetic field. This behavior can be explained as; when a magnetic field it is expected that the acting magnetic force on the electron particle motion in the parallel direction of the electric field increases and consequently its kinetic energy increases the discharge current. Therefore, the micro-discharge presented more homogeneous in space between the electrodes. Consequently, the excitation and photo emission processes becomes higher than that of ionization case, which lead to a more luminous zone higher than that without the magnetic field [42,57]. T_e is the most plasma characteristic that described the plasma state. Anyway, if we assumed that the local thermodynamic equilibrium is established in the plasma, then the number of excited atoms follows the Boltzmann distribution to determine of T_e.

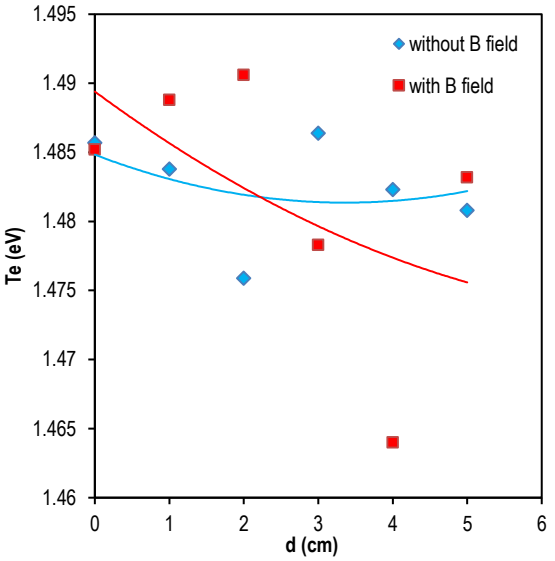

Fig. (6) The variation of electron temperature with moving distance (D) in two cases with and without magnetic field

Table (1) O II standard emission lines that used to calculate electron temperature, and their characteristics

λ (nm)	$A_{ki}g_k$ (S^{-1})	E_i (eV)	E_k (eV)
337.714	2.66E+08	25.28562	28.95584
380.2984	1.36E+08	26.56109	29.82035
734.6895	1.72E+07	29.06224	30.74935
357.3763	2.01E+05	30.74935	34.21765

Using Eq. (1) with the data that listed in table (1), the electron temperature was evaluated in the presence and absence of the magnetic field as shown in Fig. (6). From this figure one can observed that, the variation of T_e with distance D shown inverse behavior when the magnetic field was applied. The variation of T_e behavior with the distance D was due to the variation of the surface area of the powered electrode with the changing of the distance D. this

result means that the characteristics of micro-discharge changed in the presence of the parallel magnetic field. In addition, the data shown also because of the magnetic confinement, the electron temperature decreases with increase of the distance D. Anyway, the spectroscopic atomic lines that emitted from the plasma represent the most reliable technique for determining of the electron number density (n_e). Using stark effect based for λ=380.298nm and Eq. (2) can be calculated electron number density at various horizontal distance utilized the values (ω_m =0.418Å for peak λ=380.298nm) [58]. Figure (7) displays the variation of n_e with horizontal distance in two cases with and without magnetic field. It is pointed out from this figure, without magnetic field the electron number density increased with increases of the horizontal distance. This result agree with reference [56]. While when the magnetic field was applied in the parallel direction of electric field, the data detected the reduction in the electron number density with increases of the horizontal distance (i.e. reduces of the surface area of powered electrode).

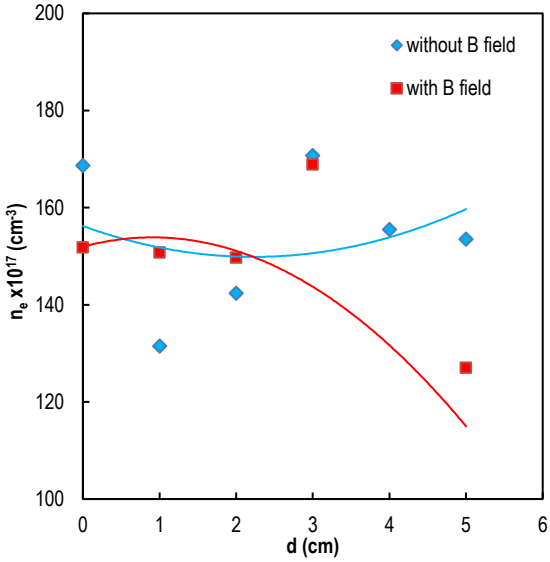

Fig. (7) Variation of electron number density with moving distance for with and without magnetic field at 9kHz frequency

Since the presence of the magnetic field has much effect on the surface electrons, the electron diffusion was increases which cause to reduce in the electron number density. As well as, the decrease in the electron surface dissipation is revealed in the phenomenon that the intensity of reverse discharges was significantly enhanced by the parallel magnetic field. The dissipation of energetic electrons in the heads of the avalanche was reduced by the parallel magnetic field [44]. Figure (8) illustrated the effect of the magnetic field on the variation of Debye length (λ_D) with the horizontal distance at atmospheric pressure. One can noticed from this figure, the presence of the magnetic field causes to change the behavior of the Debye length with increases of horizontal distance (D). One can detected that the micro-discharge channel becomes wider in the present of the magnetic field.

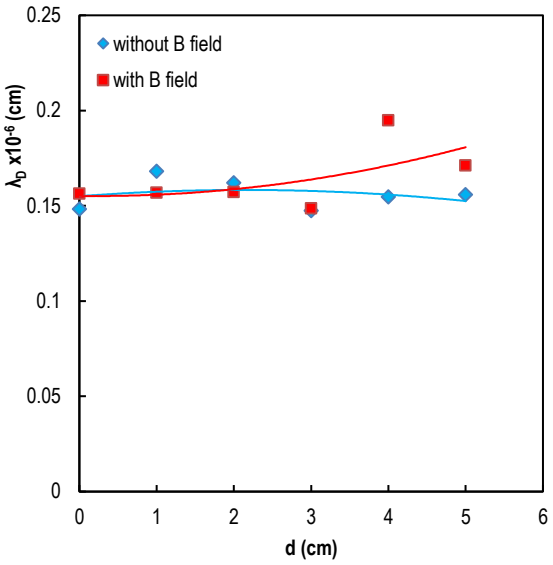

Fig. (8) The effect of the magnetic field on the variation of λ_D as function of horizontal distance at atmospheric pressure

Finally, figure (9) demonstrated the influence of the magnetic field on the number of charged particles in the Debye sphere (N_D) versus the horizontal distance. On can observe that, when the magnetic field is not exist, the plasma parameter is approximately not affect by varying of the horizontal distance. On the other hand, when the magnetic field is applied the experimental curve of N_D display that there is slightly increase of N_D when the horizontal distance increases greater than 3 cm. this behavior of N_D means that the magnetic field causes the variation of micro-discharge structure and the structure of the micro-discharge also variation with horizontal distance.

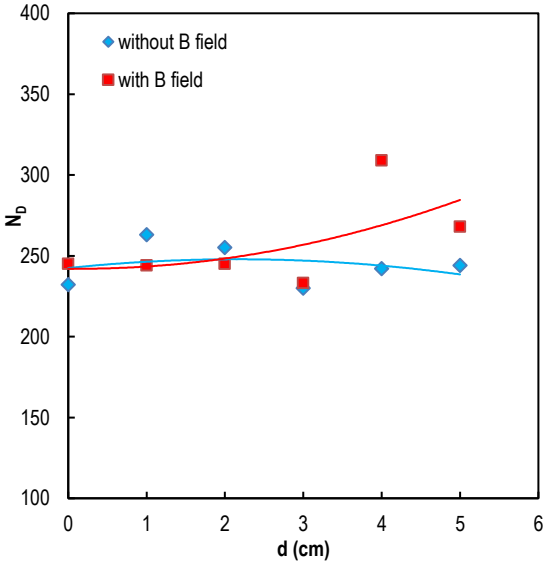

Fig. (9) Influence of the magnetic field on the variation of the plasma parameter as function of the horizontal distance at

atmospheric pressure

5. Conclusion

In the current work, the experimental data investigated that there is a significant effect of electrode area on the properties of the micro-discharge that formed in the DBD actuator in the presence and absence of the magnetic field. The presence of parallel magnetic field will effect on the micro-discharge characteristics in all horizontal distance. There is a significant the impact of the parallel magnetic field on the surface electrons.

References

[1] [1] A. Kumar et al., "Plasma Polymerization: Electronics and Biomedical Application", in "Plasma Science and Technology for Emerging Economies", Springer (2017) 593-657.

[2] [2] A.K. Abd and Q.A. Abbas, "Surface Treatment of Epoxy/Al Composite by Dielectric Barrier Discharge (DBD) at Atmospheric Pressure", *Iraqi J. Sci.*, 64(6) (2023) 2867-2876.

[3] [3] S.F. Khaleel and Q.A. Abbas, "Effect of dielectric barrier discharge on conductive properties for epoxy/copper composite", *J. Phys.: Conf. Ser.*, 2114(1) (2021) 012042.

[4] [4] D.P. Subedi et al., "Treatment of water by dielectric barrier discharge", *J. Sci. Technol. Tropics*, 5(2) (2009) 117-123.

[5] [5] U. Kogelschatz, B. Eliasson and W. Egli, "Dielectric-barrier discharges. Principle and applications", *Le J. de Phys. IV*, 7(C4) (1997) C4-47.

[6] [6] L.R. Grabowski, "Pulsed corona in air for water treatment", PhD thesis, Eindhoven University of Technology, Netherlands (2006).

[7] [7] H. Ukhtiyah, K. Kusumandari and T.E. Saraswati, "Effect of Dielectric Barrier Discharge (DBD) plasma treatment in drinking water on physical, chemical, and biological parameters", *J. Phys.: Conf. Ser.*, 2498(1) (2023) 012017.

[8] [8] T. Shibata and H. Nishiyama, "Water treatment by dielectric barrier discharge tube with vapor flow", *Int. J. Plasma Enviro. Sci. Technol.*, 11(1) (2017) 112-117.

[9] [9] S.-H. Ji et al., "Effects of high voltage nanosecond pulsed plasma and micro DBD plasma on seed germination, growth development and physiological activities in spinach", *Archiv. Biochem. Biophys.*, 605 (2016) 117-128.

[10] [10] A. Gómez-Ramírez et al., "Surface chemistry and germination improvement of Quinoa seeds subjected to plasma activation", *Sci. Rep.*, 7(1) (2017) 5924.

[11] [11] L. Sivachandiran and A. Khacef, "Enhanced seed germination and plant growth by atmospheric pressure cold air plasma: combined effect of seed and water treatment", *RSC Adv.*, 7(4) (2017) 1822-1832.

[12] [12] Y. Liu, Z. Fang and L. Cai, "Improving hydrophilicity of polypropylene film using atmospheric pressure plasma jet in argon", *High Voltage Eng.*, 38(5) (2012) 1141-1149.

[13] [13] T. Shao et al., "Surface modification of polyimide films using unipolar nanosecond-pulse DBD in atmospheric air", *Appl. Surf. Sci.*, 256(12) (2010) 3888-3894.

[14] [14] N.Y. Babaeva, W. Tian and M.J. Kushner, "The interaction between plasma filaments in dielectric barrier discharges and liquid covered wounds: electric fields delivered to model platelets and cells", *J. Phys. D: Appl. Phys.*, 47(23) (2014) 235201.

[15] [15] A.V. Nastuta et al., "Stimulation of wound healing by helium atmospheric pressure plasma treatment", *J. Phys. D: Appl. Phys.*, 44(10) (2011) 105204.

[16] [16] A. Yang et al., "Characteristics of the atmospheric pressure argon plasma jet", *High Voltage Eng.*, 38(7) (2012) 1763-1769.

[17] [17] B. Jiang et al., "Review on electrical discharge plasma technology for wastewater remediation", *Chem. Eng. J.*, 236 (2014) 348-368.

[18] [18] A.Z. Zain et al., "Development of ozone reactor for medicine base on dielectric barrier discharge (DBD) plasma", *J. Phys.: Conf. Ser.*, 1153(1) (2019).

[19] [19] M. Restiwijaya et al., "New development of double dielectric barrier discharge (DBD) plasma reactor for medical", *J. Phys.: Conf. Ser.*, 1170(1) (2019).

[20] [20] J. Hu et al., "Dielectric barrier discharge in analytical spectrometry", *Appl. Spectro. Rev.*, 46(5) (2011) 368-387.

[21] [21] P. Vanraes et al., "Study of an AC dielectric barrier single micro-discharge filament over a water film", *Sci. Rep.*, 8(1) (2018) 10919.

[22] [22] U. Kogelschatz, "Dielectric-barrier discharges: their history, discharge physics, and industrial applications", *Plasma Chem. Plasma Process.*, 23 (2003) 1-46.

[23] [23] M. Gad-el-Hak, "Flow control", Cambridge University Press (1989) 261-293.

[24] [24] J.R. Roth and X. Dai, "Optimization of the aerodynamic plasma actuator as an electrohydrodynamic (EHD) electrical device", *44th AIAA Aerospace Sci. Meet. Exhibit* 9-12 January 2006, Reno, Nevada (AIAA 2006-1203).

[25] [25] K.P. Singh and S. Roy, "Impedance matching for an asymmetric dielectric barrier discharge plasma actuator", *Appl. Phys. Lett.*, 91(8) (2007) 081504.

[26] [26] M. Neumann et al., "Determination of the phase-resolved body force produced by a dielectric barrier discharge plasma actuator", *J. Phys. D: Appl. Phys.*, 46(4) (2012) 042001.
[27] [27] Q. Sun et al., "Study on Characteristics of an AC Sliding Discharge Plasma Actuator Operating at Different Pressures", *MDPI Actuators*, 12(1) (2023) 34.
[28] [28] J. Roth, D. Sherman and S. Wilkinson, "Boundary layer flow control with a one atmosphere uniform glow discharge surface plasma", *36th AIAA Aerospace Sci. Meet. Exhibit*, 12-15 January 1998, Reno, Nevada (AIAA 98-0328).
[29] [29] T.C. Corke, M.L. Post and D.M. Orlov, "Single dielectric barrier discharge plasma enhanced aerodynamics: Physics, modeling and applications", *Exper. Fluids*, 46 (2009) 1–26.
[30] [30] N. Benard and E. Moreau, "Electrical and mechanical characteristics of surface AC dielectric barrier discharge plasma actuators applied to airflow control", *Exper. Fluids*, 55 (2014) 1-43.
[31] [31] M. Kotsonis, "Diagnostics for characterisation of plasma actuators", *Measur. Sci. Technol.*, 26(9) (2015) 092001.
[32] [32] N. Benard and E. Moreau, "Role of the electric waveform supplying a dielectric barrier discharge plasma actuator", *Appl. Phys. Lett.*, 100(19) (2012) 193503.
[33] [33] T. Abe et al., "Experimental study for momentum transfer in a dielectric barrier discharge plasma actuator", *AIAA J.*, 46(9) (2008) 2248-2256.
[34] [34] J. Soni and S. Roy, "Low pressure characterization of dielectric barrier discharge actuators", *Appl. Phys. Lett.*, 102(11) (2013) 112908.
[35] [35] A. Debien, N. Benard and E. Moreau, "Streamer inhibition for improving force and electric wind produced by DBD actuators", *J. Phys. D: Appl. Phys.*, 45(21) (2012): 215201.
[36] [36] F.O. Thomas, A. Kozlov and T.C. Corke, "Plasma actuators for cylinder flow control and noise reduction", *AIAA J.*, 46(8) (2008) 1921-1931.
[37] [37] Y. Li, X. Zhang and X. Huang, "The use of plasma actuators for bluff body broadband noise control", *Exper. Fluids*, 49 (2010) 367-377.
[38] [38] K. Shimizu and M. Blajan, "Dielectric barrier discharge microplasma actuator for flow control", Actuators, IntechOpen (London, 2018), doi: 10.5772/intechopen.75802.
[39] [39] J. Zito et al., "Microscale dielectric barrier discharge plasma actuators: Performance characterization and numerical comparison", *43rd AIAA Plasma Dynam. Lasers Conf.*, 25-28 June 2012, New Orleans, Louisiana (AIAA 2012-3091)
[40] [40] S. Pekárek, "Experimental study of nitrogen oxides and ozone generation by corona-like dielectric barrier discharge with airflow in a magnetic field", *Plasma Chem. Plasma Process.*, 37(5) (2017) 1313-1330.
[41] [41] J.Y. Park et al., "NO_x removal using DC corona discharge with magnetic field", *Combus. Sci. Technol.*, 133(1-3) (1998) 65-77.
[42] [42] Y. Liu et al., "The impacts of magnetic field on repetitive nanosecond pulsed dielectric barrier discharge in air", *Phys. Plasmas*, 23(11) (2016) 113508.
[43] [43] C. Wang et al., "Surface treatment of polypropylene films using dielectric barrier discharge with magnetic field", *Plasma Sci. Technol.*, 14(10) (2012) 891.
[44] [44] Y. Liu et al., "Effect of parallel magnetic field on repetitively unipolar nanosecond pulsed dielectric barrier discharge under different pulse repetition frequencies", *Phys. Plasmas*, 25(3) (2018) 033519.
[45] [45] A.K. Bard and Q.A. Abbas, "Influence of Cylindrical Electrode Configuration on Plasma Parameters in a Sputtering System", *Iraqi J. Sci.*, 63(8) (2022) 3412-3423.
[46] [46] A.K. Abd and Q.A. Abbas, "Spectral Analysis of the Effects of Variation in Electrodes' Area for Dielectric Barrier Discharge Actuator", *Iraqi J. Sci.*, 64(4) (2023) 1691-1703.
[47] [47] A.M. El Sherbini et al., "Measurements of plasma electron temperature utilizing magnesium lines appeared in laser produced aluminum plasma in air", *Opt. Photon. J.*, 2(04) (2012) 278.
[48] [48] M.M. Kahim, Q.A. Abbas and M.R. Abdulameer, "Study of Some Plasma Characteristics in Dielectric Barrier Discharge (DBD) System", *Iraqi J. Sci.*, 63(5) (2022) 2048-2056.
[49] [49] M.U. Hussein and T.H. Khalaf, "The effect of Dielectric Thickness on Dielectric Barrier Discharge properties at Atmospheric Pressure", *Eng. Technol. J.*, 33(6B) (2015) 1102-1109.
[50] [50] F.F. Chen, **"Introduction to Plasma Physics and Controlled Fusion"**, Springer (2016).
[51] [51] Q.A. Abbas, F.Y. Hadi and S.S. AL-Awadi, "Modified Bohm Diffusion equation in Q-Machine", *Baghdad Sci. J.*, 8 (2011) 339-344.
[52] [52] H.Q. Farag and S.J. Kadhem, "Study the Effect of Dielectric Barrier Discharge (DBD) Plasma on the Decomposition of Volatile Organic Compounds", *Iraqi J. Phys.*, 20(4) (2022) 45-53.
[53] [53] R.S. Mohammed, K.A. Aadim and K.A. Ahmed, "Spectroscopy diagnostic of laser intensity effect on Zn plasma parameters generated by Nd: YAG laser", *Iraqi J. Sci.*, 63(9) (2022) 3711-3718.

[54] [54] S. Iordanova and I. Koleva, "Optical emission spectroscopy diagnostics of inductively-driven plasmas in argon gas at low pressures", *Spectrochimica Acta B: Atom. Spectro.*, 62(4) (2007) 344-356.
[55] [55] B.M. Ahmed, "Plasma parameters generated from iron spectral lines by using LIBS technique", *IOP Conf. Ser.: Mater. Sci. Eng.*, 928(7) (2020) 072096.
[56] [56] S.F. Khaleel and Q.A. Abbas, "Influence of Dielectric Media on the Plasma Characteristics in DBD Discharge", *Iraqi J. Sci.*, 63(6) (2022) 2470-2481.
[57] [57] A. El-Zein et al., "The Characteristics of Dielectric Barrier Discharge Plasma under the Effect of Parallel Magnetic Field", *IEEE Trans. Plasma Sci.*, 48(4) (2020) 1022-1029.
[58] [58] N. Konjević et al., "Experimental Stark widths and shifts for spectral lines of neutral and ionized atoms (a critical review of selected data for the period 1989 through 2000)", *J. Phys. Chem. Ref. Data*, 31(3) (2002) 819-927.

